



Research Publication Repository

<http://publications.wehi.edu.au/search/SearchPublications>

This is the author's version of the work. It is posted here by permission of the AAAS for personal use, not for redistribution.

Publication details:	Trevelyan SJ, Brewster JL, Burgess AE, Crowther JM, Cadell AL, Parker BL, Croucher DR, Dobson RCJ, Murphy JM, Mace PD. Structure-based mechanism of preferential complex formation by apoptosis signal-regulating kinases. <i>Science Signaling</i> . 2020 13(622)
Published version is available at:	https://doi.org/10.1126/scisignal.aay6318

Changes introduced as a result of publishing processes such as copy-editing and formatting may not be reflected in this manuscript.

Structure-based mechanism of preferential complex formation by Apoptosis Signal-regulating Kinases.

Sarah J. Trevelyan¹, Jodi L. Brewster¹, Abigail E. Burgess¹, Jennifer M. Crowther^{2†}, Antonia L. Cadell³, Benjamin L. Parker⁴, David R. Croucher^{3,5,6}, Renwick C.J. Dobson^{2,7}, James M. Murphy^{8,9}, Peter D. Mace^{1,*}

¹ Biochemistry Department, School of Biomedical Sciences, University of Otago, P.O. Box 56, 710 Cumberland St., Dunedin 9054, New Zealand

² Biomolecular Interaction Centre, School of Biological Sciences, University of Canterbury, Christchurch, New Zealand

³ The Kinghorn Cancer Centre, Garvan Institute of Medical Research, Sydney, New South Wales 2010, Australia

⁴ Department of Physiology, School of Biomedical Sciences, The University of Melbourne, Parkville, Victoria 3010, Australia

⁵ St Vincent's Hospital Clinical School, University of New South Wales, Sydney, New South Wales, 2052, Australia

⁶ School of Medicine and Medical Science, University College Dublin, Belfield, Dublin 4, Ireland

⁷ Department of Biochemistry and Molecular Biology, Bio21 Molecular Science and Biotechnology Institute, University of Melbourne, Parkville, Victoria 3010, Australia

⁸ The Walter and Eliza Hall Institute of Medical Research, Parkville, Victoria 3052, Australia

⁹ Department of Medical Biology, University of Melbourne, Parkville, Victoria 3010, Australia

† Present address: Institute of Quantitative Biology, Biochemistry and Biotechnology, University of Edinburgh, Edinburgh, United Kingdom.

* Corresponding author. Email: peter.mace@otago.ac.nz

Abstract

Apoptosis signal-regulating kinases (ASK1, ASK2, and ASK3) are activators of the P38 and Jun N-terminal kinase (JNK) mitogen-activated protein (MAP) kinase pathways. ASK1–3 form oligomeric complexes known as ASK signalosomes that initiate signaling cascades in response to diverse stress stimuli. Here we demonstrated that oligomerization of ASK proteins is driven by previously uncharacterised sterile-alpha motif (SAM) domains that reside at the C-terminus of each ASK protein. SAM domains from ASK1–3 exhibited distinct behaviors, with the SAM domain of ASK1 forming unstable oligomers, that of ASK2 remaining predominantly monomeric, and that of ASK3 forming a stable oligomer even at low concentration. In contrast to their behavior in isolation, the ASK1 and ASK2 SAM domains preferentially formed a stable heterocomplex. The crystal structure of the ASK3 SAM domain, small-angle X-ray scattering, and mutagenesis suggested that ASK3 oligomers and ASK1-ASK2 complexes formed discrete quasi-helical rings through interactions between the mid-loop of one molecule and the end-helix of another molecule. Preferential ASK1-ASK2 binding was consistent with mass spectrometry showing that full-length ASK1 formed heterooligomeric complexes incorporating high amounts of ASK2. Accordingly, disrupting the association between SAM domains impaired ASK activity in the context of electrophilic stress induced by 4-hydroxy-2-nonenal (HNE). These findings provide a structural template for how ASK proteins assemble foci that drive inflammatory signaling and reinforce the notion that strategies targeting ASK proteins should consider the concerted actions of multiple ASK family members.

Introduction

Mitogen-activated protein kinase (MAPK) cascades are ubiquitous in eukaryotes as a means of sensing and responding to stressors. In humans, the Jun N-terminal kinase (JNK) and P38 MAP kinases are activated by upstream MAP kinase kinases (MAP2Ks), which are in turn activated by a diverse group of MAP kinase kinase kinases (MAP3Ks). Although the activation of both MAPKs and MAP2Ks by phosphorylation is well understood, MAP3Ks are less well characterised. This imbalance is likely because MAPKs and MAP2Ks are activated by relatively well-defined upstream kinases, whereas stress-activated MAP3Ks must recognise and respond to a wide range of stressors, so have more diverse regulation that remains to be characterised at the molecular level.

Apoptosis signal-regulated kinases (ASKs) are a group of MAP3Ks that respond to various chemical, physical, and inflammatory stimuli. In humans there are three ASK-family kinases: ASK1, ASK2, and ASK3 (also known as MAP3K5, MAP3K6, and MAP3K15, respectively). ASK1 has been intensively studied following the initial discovery of its activation in response to tumor necrosis factor (TNF), promoting cell death (1). Subsequently, roles for all three ASK proteins have been defined in various biological pathways and disease states. For instance, a role for ASK1 is now well established in the response to oxidative stress and inflammatory cytokines (2, 3). ASK1 and ASK2 are required for effective responses to viral infection (4–6), to prime inflammasomes containing nucleotide-binding domain and leucine-rich repeat-containing (NLR) proteins following challenge by bacterial infection (7), and together mediate neutrophilic dermatitis (8). In simplified terms, it appears that ASK1 and ASK2 in isolation can each promote some amount of P38 and JNK activation and stress response, but their concerted action generates a broader inflammatory response, and, in some cases, cell death. ASK3 apparently has a more specialised role in sensing and responding to osmotic pressure and regulation of blood pressure, specifically in the kidney upstream of the serine-threonine kinase WNK1 [With no lysine (K)] (9).

ASK1 has generated significant interest due to the relevance of ASK1 to disease and the availability of specific inhibitors, in particular Selonsertib (10). Activating mutations of ASK1 occur in melanoma (11), and inhibition of ASK1 has shown benefit in gastric cancers (12, 13). Most notably, ASK1 is a relevant target in non-alcoholic steatohepatitis (NASH; (14)). ASK1 inhibition with Selonsertib has shown promising results up to phase-two clinical trials (10), and other inhibitors derived from Selonsertib also reduce fibrosis caused by kidney inflammation (15). Despite their clinical relevance, a structural understanding of ASK protein complexes beyond the well-conserved catalytic kinase domain is limited. The ASK1 kinase domain structure was first solved in 2007 (16), and subsequently crystal structures of small-molecule inhibitors in complex with the kinase have become available. However, ASK1–3 are each greater than 1300 amino acids in length, and the precise mechanisms linking their conserved architecture—wherein the central kinase domain is flanked by large N- and C-terminal regulatory domains (Fig. 1A)—to kinase activity remain unclear.

The current model of ASK1 regulation invokes constitutive oligomerisation mediated through the C-terminal region, in parallel with stimuli-dependent regulation of ASK signaling through the N-terminus (17). Many of the signaling molecules that are proposed to regulate stress-induced activation of ASK1 interact through its N-terminal domains. There are further outstanding questions regarding the interaction of regulatory and oligomerising domains of ASK proteins. It is not clear if regulation of substrate recruitment and priming, through a

domain just N-terminal to the kinase (18), occur in an intra- or inter-molecular manner. Likewise it is not known if dimers reported for the isolated kinase domain of ASK1 impact kinase function in the context of full-length protein (16). Moreover, the C-terminal region of ASK proteins is clearly important for signalosome formation and activity, but the structural mechanism of assembly and how this relates to oligomerisation of different ASK-type kinases remains to be determined.

Here we present the crystal structure of the C-terminal domain of ASK3, which adopts a sterile alpha motif (SAM) fold, a structure classically shown to mediate protein-protein interactions that had not previously been described in ASK proteins. Interrogating the behavior of C-terminal domains of ASK1–3 using various methods in solution and full-length ASK1 and ASK2 in cells uncovered distinct behaviours of the C-terminal domains from the three ASK proteins, which impact protein complex assembly and activity. These data provide a structural basis for previous observations regarding ASK protein oligomerisation and functional cooperativity of ASK proteins in various biological settings.

Results

ASK1–3 C-terminal domains have divergent oligomerisation propensities

Sequences C-terminal to the ASK1 kinase domain are known to play roles in binding regulatory proteins (19, 20) and facilitating interactions between ASK proteins to generate oligomeric ASK signalosomes (17). Although a coiled-coil region is predicted near the C-terminus of each ASK protein, the precise structural architecture of the C-terminal portion of ASK proteins is unclear. To gain insight into the mechanism of oligomerisation, we expressed C-terminal fragments from ASK1, ASK2, and ASK3. Regions of ASK1(1039–1374), ASK1(1237–1374), ASK2(988–1288), and ASK2(1156–1288) that incorporate the predicted C-terminal coiled-coil (residues 1245–1285 in ASK1) were all highly insoluble when expressed alone or co-expressed, in either *Escherichia coli* or Sf9 insect cells. In contrast, shorter constructs comprising ASK1(1290–1374), ASK2(1216–1288), and ASK3(1241–1313) (9.8, 8.2, 8.5 kDa, respectively) all readily expressed in a soluble form in *E. coli*.

Assessment of the soluble C-terminal portions of ASK proteins using analytical size-exclusion chromatography (SEC) and analytical ultracentrifugation (AUC) revealed that these smaller fragments themselves had the ability to form oligomers. However, each exhibited a distinct behaviour. SEC showed an unstable ASK1 oligomer that existed in an equilibrium between multiple oligomeric states, even at concentrations as high as 200 μ M (Fig. 1B). Sedimentation velocity AUC corroborated this result, with 15–150 μ M ASK1 forming concentration-dependent oligomers of two distinct sizes (Fig. 1C; table S1). In comparison, ASK2 was a single species on SEC, eluting with an apparent mass consistent with a monomer (Fig. 1B). AUC also showed that ASK2 existed almost exclusively as a monomer, only exhibiting a minor dimer species when analysed at a concentration of 365 μ M (3 mg/mL; table S1). Finally, ASK3 formed a large and stable oligomer with an apparent mass of \sim 54 kDa, as assessed from molecular weight standards (Fig. 1B). Analysis of ASK3 using AUC suggested a single oligomeric state over a 10-fold concentration range (Fig. 1C; table S1), allowing for a good mass estimation from the sedimentation velocity experiment. When measured between 0.15 and 1.5 mg/mL, the calculated molecular weight values fell in a range between 41.3 and 47 kDa, generally between the mass of an ASK3 pentamer or hexamer, which would have a theoretical mass of \sim 42.5 kDa or 51 kDa respectively.

To further interrogate the soluble C-terminal domains of ASK1–3, we analysed their amino acid sequences using sequence profile matching (21), which suggested similarity to SAM domains from various proteins—including P63, Tankyrase, and the yeast MAPK-related proteins Ste11 and Ste50 (22–25). Although there has been some reference to a predicted SAM domain in ASK1 (26), the SAM designation does not appear in major fold-prediction databases, and the same region has also been noted to contain a ubiquitin-like sequence motif (26, 27). Because SAM domains are versatile interaction modules that mediate both protein-protein and protein-DNA interactions, a C-terminal SAM domain would make an ideal candidate to mediate ASK oligomer formation.

The ASK3 C-terminal domain is a Sterile-Alpha Motif (SAM) domain

To gain further insight into the oligomerisation mechanism of the ASK1–3 C-terminal domains we pursued structural studies. Crystallisation trials of the soluble C-terminal domains from the three ASK proteins yielded crystals of ASK3(1241–1313), from which the structure was solved using a combination of single-isomorphous replacement plus anomalous scattering (SIRAS) and molecular replacement with single-wavelength anomalous dispersion (MR-SAD) (Fig. 2A). The structure was refined against native diffraction data to a resolution of 1.8 Å and has excellent geometric parameters (table S2). There are three molecules of ASK3(1241–1313) in the asymmetric unit, with the ASK3 polypeptide chain defined from residues 1241–1308 in two molecules, and 1241–1305 in the third molecule.

Consistent with bioinformatic prediction, the C-terminal domain of ASK3 adopted the classical five-helix fold of the SAM domain. The sequence of ASK1 and ASK2 are 53 and 37 % identical, respectively, in the equivalent regions to the solved structure of ASK3 (Fig. 2B). The highest amounts of conservation are concentrated in hydrophobic core residues, and both ASK1 and ASK2 are also predicted to contain five helices. Therefore, we propose that the three ASK proteins all possess a similar SAM-fold at their C-terminus. Although we grew crystals of the SAM domain of ASK1, the crystals did not diffract sufficiently for structure determination.

The ASK3 SAM domain oligomerises through the ML-EH interface

With three ASK3 molecules in the asymmetric unit, there are several interfaces through which ASK oligomers may form. Based on the crystal contacts, we observed three possibilities (fig. S1): the mid-loop: end-helix (ML-EH) interaction that has been observed for SAM domains from diverse protein families (Fig. 2, A and C)(28); a symmetrical interaction formed by the C-terminal helix of ASK3; and a symmetrical interaction through the surface of $\alpha 1$ and $\alpha 2$ with a neighboring asymmetric unit. We generated a suite of mutant ASK3 SAM domains to deduce which of the interfaces observed in the crystal lattice corresponded to the oligomerisation interface in solution. Examining mutants by SEC, we identified the ML-EH interaction as the crucial site for oligomerisation. The D1279Q mutant, which disrupts the ML-EH interaction, eluted with an apparent mass of 13 kDa, close to that of a monomer (Fig. 2, C and D). Mutation of residues at the C-terminal helix led to ambiguous results. The ASK3(Q1304A) mutant designed to disrupt the hydrogen bond between Gln¹³⁰⁴ and Tyr¹³⁰⁰ oligomerized in an equivalent manner to the wild-type ASK3 SAM; whereas mutations of Tyr¹³⁰⁰ (Y1300Q and Y1300A), which is close to the core of the SAM domain, shifted towards a smaller apparent mass but had broadened appearance (fig. S2A). Mutation that affect the $\alpha 1$ - $\alpha 2$ interface (V1262N) did not disrupt the oligomer (fig. S2B), indicative of purely crystallographic contacts through $\alpha 1$ - $\alpha 2$. Thus, we cannot completely discount the role of the C-terminal-helix interaction, but the ML-EH interaction appears to be crucial because a

single point mutant at this interface most effectively disrupted the ASK3 complex. To further test this hypothesis, we introduced an additional mutation on the opposite side of the ML-EH interface, ASK3(C1291E), and tested its ability to oligomerise using SEC coupled to multiple angle light scattering (SEC-MALS). By SEC-MALS, ASK3(C1291E) had a calculated mass of 8.5 kDa (Fig. 2E), close to its theoretical monomer mass of 8.7 kDa and consistent with an indispensable role for ML-EH interface formation.

To extend the model of SAM oligomerisation from ASK3 to ASK1 and ASK2, we made mutations of the ML-EH interface and C-terminal helix to ASK1. The ASK1 ML-EH interface mutant ASK1(C1360E) eluted as a single sharp peak at a smaller apparent mass than the wild-type protein, whereas the C-terminal helix mutation of ASK1 (F1369Q) behaved in an identical manner to wild-type protein (fig. S3A). Upon SEC-MALS, ASK1(C1360E) had a calculated mass of 13.4 kDa (fig. S3C), close to the theoretical monomeric mass of 10.3 kDa, and indicative of the ML-EH interface being the key driver of ASK1 oligomerisation. The wild-type ASK2 SAM domain had a calculated mass of 8.6 kDa in SEC-MALS, even though it eluted in a notably different position relative to ASK1 and ASK3 monomers (fig. S3D). Relatedly, it is worth noting that the residues at the end of the C-terminal helix of ASK1–3 are relatively divergent, which could impact the hydrodynamic radius, stability of the helix, and the ML-EH interface (fig. S3B). From these data, we conclude that weak oligomerisation of the ASK1 SAM domain and stable oligomer formation by the ASK3 SAM domain requires the ML-EH interface, because single point mutants that disrupt the ML-EH behave as a monomeric proteins.

ASK1-ASK2 form heterotypic complexes through the ML-EH interface

ASK1 and ASK2 have previously been reported to associate through their C-terminal domains (4), and endogenous ASK1 and ASK2 have been reported to exist in complex with one another at an equal ratio (29). We next sought to test whether such heterotypic association could be driven through the isolated SAM domains of each ASK protein. As an initial measure, we prepared glutathione S-transferase (GST)-fused forms of the SAM domain from each ASK protein and tested the ability of each to pull down the other respective SAM domains. We observed that the ASK1 SAM domain only associated with the ASK2 domain, but not untagged ASK1, or ASK3 SAM (Fig. 3A). The ASK2 SAM domain was not able to pull down its own untagged form—consistent with its monomeric behaviour in solution (Fig. 3A)—but readily pulled down ASK1 and ASK3 (Fig. 1A). ASK3 on the other hand showed only weak interactions with untagged SAM domains from any ASK protein (Fig. 3A). The scarcity of interactions by ASK3 could be because ASK3 readily forms oligomers over a range of concentrations (Fig. 1C), and thus GST-ASK3 SAM is unable to incorporate additional untagged ASK3 SAM.

To further characterise the heterotypic association between ASK1 and ASK2, we used sedimentation velocity AUC (Fig. 3B; table S1). Consistent with the GST pulldowns, the ASK1-ASK2 mixture readily associated and formed a defined oligomer. Such behaviour was in marked contrast to the weak homotypic association of ASK1 and ASK2 SAM domains, and suggests that the two domains from ASK1 and ASK2 preferentially oligomerize into a larger complex. This behaviour suggests that the SAM domains of each protein contribute markedly to the heteromeric ASK1-ASK2 complexes previously reported (4–8, 29).

To ascertain if ASK1-ASK2 hetero-oligomers also use the ML-EH interface, we first tested the role of the conserved cysteine residue (Cys¹³⁶⁰ in ASK1 and Cys¹²⁶⁸ in ASK2) that was previously shown to be essential for ASK3 oligomerisation and for weak ASK1

oligomerisation. GST pulldown experiments clearly showed that mutating either Cys¹³⁶⁰ of ASK1 or Cys¹²⁶⁸ of ASK2 to glutamate ablated binding to the wild-type form of its partner protein (Fig. 3C). To gain further information on the oligomerisation status of these mutant proteins, we performed analytical SEC (Fig. 3, D and E). We observed that ASK1(C1360E) showed no higher-order complex formation when combined with wild-type ASK2 SAM domain, having precisely the equivalent elution time as when it was analysed by itself. The corresponding mutation in ASK2(C1268E) reinforced this observation, with the mixture of ASK1–ASK2(C1268E) SAM domains barely distinguishable from their isolated elution positions, showing no sign of higher-order complex assembly. Together, these interaction studies show that the SAM domains from ASK1 and ASK2 exhibit a preference to form heterotypic—rather than homotypic—higher-order oligomers through the ML-EH interfaces of each protein.

SAM-mediated oligomers regulate activity and stoichiometry in cells

Having established that disrupting the ML-EH interface of either ASK1 or ASK2 abrogates SAM domain heterocomplexes, we sought to test the effects on activity. We transfected wild-type full-length and disruptive mutants ASK1(C1360E) and ASK2(C1268E) into HEK293FT cells and challenged cells with the prototypic electrophilic stressor 4-hydroxy-2-nonenal (HNE). As expected, HNE treatment of cells overexpressing wild-type full-length ASK1 induced phosphorylation of ASK1, indicating activation of kinase activity (Fig. 4, A and B). The oligomer-disrupted mutant ASK1(C1360E) showed decreased relative phosphorylation upon HNE stimulation, characteristic of impaired activity (Fig. 4, A and B). There was no phosphorylation detected when either wild-type ASK2 or the C1268E mutant was transfected alone, despite similarity of amino acid sequences in the activation loop epitope of ASK1 and ASK2 (4). When transfected together, wild-type ASK1 and ASK2 show lower basal amounts of kinase activity, which was activated by HNE (Fig. 4, A and B). Strikingly, transfection of ASK1(C1360E) and ASK2(C1268E) together abrogated basal phosphorylation, which was not stimulated by HNE treatment (Fig. 4, A and B). When we combined either wild-type ASK1 with ASK2(C1268E), or ASK1(C1360E) with wild-type ASK2, we observed low amounts of ASK1 phosphorylation upon challenge with HNE (fig. S4). This result likely reflects that ASK1 and ASK2 can interact in a head-to-tail manner and that either ASK protein can provide an ML or EH interface. Therefore, a single ASK1 point mutant is still capable of forming at least heterodimers in the context of full-length proteins in cells. From these experiments, we can conclude that oligomerisation of ASK proteins through their SAM domains is a core feature of active signaling complex formation, which can be disrupted by the introduction of point mutations that disrupt the ML-EH interfaces of both ASK1 and ASK2.

Elegant endogenous mass spectrometry studies have previously shown that ASK1 associates with near-stoichiometric amounts of ASK2 (29). We employed an orthogonal approach—bimolecular complementation affinity purification (BiCAP (30, 31))—to determine if stoichiometric association of ASK1-ASK2 occurs as part of larger hetero-oligomeric complex. For this system, we created two constructs of full-length ASK1 fused to the N-terminal (V1), and C-terminal (V2), portions of the Venus fluorescent protein employed in BiCAP. As such, complexes immunoprecipitated using a nanobody specific for GFP must contain at least two molecules of full-length ASK1 (Fig. 4C), rather than associating with any monomeric form of the protein, as may occur with a conventional immunoprecipitation. Partner proteins identified with multimeric ASK1 were identified by mass spectrometry. Remarkably, ASK2 was identified at an abundance of approximately

75% of ASK1 itself (Fig. 4D; table S3), even though ASK1 was overexpressed whilst ASK2 was expressed in endogenous amounts. Such a result strongly suggests a selective incorporation of near-equal ratios of ASK1 and ASK2 into higher order ASK complexes. Also of note, ASK3 was also enriched in BiCAP analysis, as were several members of the ubiquitin ligase machinery (FbxW11, UBE2N/Ubc13). ASK proteins have previously been shown to undergo regulatory ubiquitylation (20, 32, 33).

Finally, to ascertain whether the near-equal ASK1-ASK2 stoichiometry observed in cells is recapitulated by isolated SAM domains, we completed a series of analytical SEC experiments with a range of ratios of ASK1 and ASK2 SAM domains. In these experiments, near-equal ratios of ASK1 and ASK2 SAM domains (120:80, 100:100 μ M ASK1:ASK2) led to the most homogenous higher order complexes, from a range ratios tested (Fig. 4E; 200:0, 160:40, 150:50, 120:80, 100:100, 80:120, 0:200 μ M, ASK1:ASK2, respectively). Together, these results suggest that SAM domains are a major determinant of ASK oligomeric state, promoting higher order complexes with near-equal ratios of ASK1 to ASK2, that can decrease ASK kinase activity in cells when disrupted.

ASK paralogs have divergent ML-EH surfaces

The ML-EH interaction occurs in several SAM domain complexes, including both discrete heterodimeric interactions and polymeric arrays of SAM domains. To name contrasting examples, the SAM domains from CNK (connector enhancer of KSR) and HYP (Hyphen) and those from EPH and SHIP2 (SH2-containing 5'-inositol phosphatase 2) form heterodimer pairs (34, 35), and the SAM domains of the poly-ADP-ribosyltransferase TNKS (Tankyrase), ANKS3 (ankyrin repeat and SAM domain-containing 3), and DGK (diacylglycerol kinase) form left-handed helical filaments through extended ML-EH interactions (23, 24, 36, 37). Comparison of structures using the secondary structure matching (SSM) server (<https://www.ebi.ac.uk/msd-srv/ssm/>) revealed that the ASK3 SAM domain aligns well (RMSD 1.4–2 Å) with several of the aforementioned SAM domains (fig. S5). To understand the different oligomerisation propensity within ASK1–3 SAM domains, we compared sequence conservation and electrostatic potential of their ML and EH surfaces. A clear pattern emerged when modelling the ASK1 and ASK2 SAM domains based on ASK3 and mapping surface electrostatics (Fig. 5A). The ASK3 ML surface is strongly negatively charged, and the EH surface is strongly positively charged, generating a highly complementary electrostatic interaction. In contrast, the ML surface of ASK2 has a generally hydrophobic character. Paired with a mildly positive EH surface, it becomes apparent that the ASK2 ML and EH surfaces are not particularly compatible with one another, hence the ASK2 SAM domain is generally monomeric. Instead, the ASK2 ML surface appears more complementary to the EH surface of the ASK1 SAM domain (Fig. 5A), and the mildly positively charged EH surface of ASK1 is complementary to the mildly negatively charged surface of the ASK1 ML surface. Such characters could explain the observed behaviour of these domains in solution, specifically that homotypic ASK1 or ASK2 interactions are transient and limited, whereas heterotypic interactions between ASK1 and ASK2 surfaces are more complementary, readily leading to stable oligomer formation.

Although experiments in cells suggested that the ML-EH surface is crucial to ASK SAM domain function, and surface comparisons indicated a possible basis for selective oligomerisation by ASK SAM domains, an outstanding question remains: Why do ASK SAM domains form distinct soluble oligomers rather than a continuous filamentous structure observed for some other SAM domains? For example, mixing high concentrations of purified monomeric and dimeric ASK1 and ASK2 SAM domains caused the formation of a distinct

pentameric or hexameric non-filamentous oligomer observed by various measures (Fig. 1; Fig. 3), and the ASK3 SAM domain also had a defined oligomeric state in solution. In considering this question, we further analysed the crystallographic contacts in the ASK3 SAM structure, and observed a second, slightly offset ML-EH interface formed with a SAM domain from a neighbouring asymmetric unit, an interaction we term ML-EH* (Fig. 5B). The ML-EH* interaction involves effectively identical residues to those that mediate the ML-EH interaction, but the relative orientation of the interacting SAM domains differs by approximately 18° (measuring relative to the position of the $\alpha 5$ helix of the non-fixed SAM domain; Fig. 5C). This indicates that there is malleability at the interface that could affect behavior in solution, in line with other ML-EH complexes and filamentous assemblies.

ASK SAM oligomers behave as quasi-helical rings in solution

To investigate why the ASK SAM domains form higher-order oligomers of defined size we turned to small-angle X-ray scattering (SAXS). We mainly sought to determine whether the SAM domains form an extended helix or a more compressed helix or ring that may self-limit, thus giving rise to a defined oligomer. In order to estimate experimental and actual scattering of oligomers formed through the ML-EH interface we considered three basic scenarios: oligomers formed by interactions through the ML-EH interface only, by interactions through the ML-EH* interface only, or a hypothetical flexible intermediate complex represented by alternating interface types. Modelling complexes formed through either ML-EH and ML-EH* have markedly different dimensions (Fig. 6A), amplifying modest differences in the pairwise interaction (Figure 5C). Specifically, the pure ML-EH oligomer forms an extended helix with a pitch of 52 Å and 7 units per turn, the pure ML-EH* oligomer a near-symmetrical closed ring, and the mixed interface an intermediate between these two types of helices (Fig. 6A).

We collected SAXS scattering data for various relevant ASK SAM domains: the isolated ASK1 and ASK2 SAM domains, the ASK1-ASK2 oligomer, and the stable ASK3 SAM domain oligomer (**Error! Reference source not found.**). Consistent with other in-solution data, the ASK2 SAM scattering data clearly fit a monomeric model ($\chi = 0.60$; fig. S6C; table S5). The experimentally determined scattering profile for ASK1 SAM domain was evaluated against both monomeric and dimeric models, whereby the radius of gyration is intermediate between the theoretical values for the monomer ($R_g = 13.6$) and MLEH dimer ($R_g = 16.5$), consistent with a mixed population observed in AUC and size-exclusion chromatography (fig. S6, A and B; Fig. 1; table S1).

High-quality scattering data was collected for both the ASK1-ASK2 and ASK3 SAM oligomers, with the low q regions of the Guinier plots indicating homogenous, monodisperse protein samples (Fig. 6, B–E). Several conformational arrangements of pentamer, hexamer and heptamer were tested against experimentally measured scattering using CRY SOL (fig. S6, D–L; table S5; (38)). For all larger complexes, the best fits to scattering data were clearly hexameric—clarifying ambiguous estimates of molecular weight arising from SEC-MALS and AUC (Fig. 6, F–H; table S5). When considering flexibility of the ML-EH interface (Fig. 6A), the best fits for ASK1-ASK2 and ASK3 differed. The best fit for the complex formed by ASK1-ASK2 SAM domains was an intermediate helix formed by a mixture of ML-EH and ML-EH* interfaces ($\chi = 0.67$), whereas the ASK3 SAM clearly fit the most compact model tested ($\chi = 0.39$; Fig. 6H). A compact, near-closed ring, for ASK3 is consistent with D_{max} estimates for ASK3 (80 Å), relative to 100 Å for ASK1-ASK2 (Fig. 6, D and E; **Error! Reference source not found.**), and provides a clear mechanism for self-limiting

oligomerisation. Although ASK1-ASK2 oligomers are slightly more extended than ASK3 oligomers, filament formation by the ASK1-ASK2 complex is likely to be prevented through steric hindrance between neighboring SAM domains. Such a model adds to the diversity of high-order SAM domain oligomers that mediate diverse biological functions (fig. S7, A–G).

Discussion

MAP kinase signaling cascades are used throughout eukaryotes to translate external stimuli into cellular responses. Having a three-tiered phosphorylation cascade allows for both signal amplification and various levels of regulation. Whereas MAP2Ks and MAPKs are relatively well conserved, MAP3Ks are significantly more divergent in their domain structure, which is made necessary by the diverse signals to which MAP3Ks sense and respond – from proliferative signals to signals eliciting cell death. One key mechanism of MAPK regulation is scaffolding of higher order complexes, which tethers relevant proteins into coherent signaling packages (39). Protein scaffolding can also modulate the catalytic activity of kinases within MAPK pathways (40, 41). ASK proteins in humans are a three-membered sub-family of MAP3Ks that have long been known to form higher-order complexes that are inherent to their function. Here we demonstrated that ASK1–3 contain a previously uncharacterised SAM domain—a prevalent protein-protein interaction domain used throughout Eukaryota (40)—at their extreme C-termini. We found that the SAM domains from the three ASK orthologs had relatively divergent oligomerisation tendencies, even though they used the same oligomerisation surface as each other and as SAM domains from many other proteins. The preferred state of ASK1–3 SAM domains varied, but notably did not extend beyond a hexameric state by any of the measures we tested, even at very high protein concentration. Both the formation of discrete oligomers and preferential hetero-oligomer formation were notable features of ASK SAM domain complex formation.

SAM domains have been characterised as either monomeric or oligomeric (42), with oligomers generally exhibiting either pairwise dimer formation or filamentous oligomer formation through the ML-EH interface. The relative orientation between ASK3 SAM domains in our crystal structure are comparable to that seen in either discrete or filamentous SAM domain oligomers. This translates to a roughly equivalent putative helical pitch (33–53 Å) to that of classical filamentous SAM domains, such as that of Tankyrase, DGK, and others (fig. S7;(23, 24, 36, 43, 44)). However, within the crystal there is obvious flexibility at the ML-EH interface, which is in line with SAXS analysis demonstrating relatively more-, or less-extended quasi-helical structures formed by discrete ASK3 homohexamers, or ASK1-ASK2 heterohexamers. Nonetheless, it remains unclear why the ASK SAM domain oligomers are self-limiting and discrete, even at concentrations exceeding 300 μM. Although the formation of a closed hexameric-ring as a mechanism of self-limitation is a tempting proposition, strong evidence is still lacking. For instance, a near-closed ring is the best match for experimental SAXS data from the ASK3 SAM, but such a closed hexamer is not seen within the crystal structure. As the data stand, we hypothesize that either the formation of a closed ring or steric occlusion—through flexibility at the ML-EH interface or through the variable C-terminal tails of each SAM domain—cause the ASK SAM domains to form discrete, self-limiting oligomers. While this manuscript was in review, intriguing structures of the SAM domains from another inflammatory signal regulator, sterile alpha and TIR motif-containing 1 (SARM1), were reported (45, 46). The SARM1 SAM domains do in fact form a closed octameric ring, which was shown to be crucial for the ability of SARM1 to trigger neuronal death in response to injury. Although the octameric ring of SARM1 SAM

domains is also formed through the ML-EH surfaces, the geometry differs as required to accommodate the octameric arrangement (fig. S7G). Nonetheless, the analogy with SARM1 is intriguing in light of a previous study showing functional linkage between the *Caenorhabditis elegans* homologs of ASK1 and SARM1 (47).

Another clear point for future investigation is how other structural elements found in full-length ASK proteins, such as the kinase domain— (which itself has been shown to dimerize) and the predicted C-terminal coiled-coil (which is located directly N-terminal to the SAM) might influence the oligomerisation behavior of ASK1–3. Pertinent to this, the Kinase Suppressor of Ras (KSR) also contains a coiled-coil SAM (CC-SAM) domain arrangement. However, the CC-SAM of KSR is responsible for membrane association and/or scaffolding interactions with RAF MAP3Ks (48, 49) rather than higher-order oligomerisation. Challenges in expressing ASK constructs incorporating the coiled-coil region make it difficult to draw conclusions on possible membrane association of the CC-SAM domains of ASK proteins. Nonetheless, our experiments in cells clearly showed that the SAM domains play a major role in setting the stoichiometry of ASK signalosomes, because ML-EH mutants exhibited diminished stress-stimulated signaling. Previous studies of ASK1 incidentally bearing mutations (deletion or alanine mutations of Gly¹³⁵⁶ and Gly¹³⁵⁷) of a similar surface also showed abrogated signaling in response to hydrogen peroxide, supporting a crucial role of the ML-EH surface in ASK signalling (46).

With growing knowledge of the domain structures of ASK proteins, the obvious challenge is understanding how oligomerisation by the SAM at the C-terminus integrates with the raft of other interactions through their N-termini. Previously, we reported the crystal structure of the central regulatory region of ASK1—located N-terminal to the kinase domain—that links the N-terminal thioredoxin-binding domain to the kinase domain (48). A pleckstrin-homology domain within this novel fold appears to promote the phosphorylation of downstream MAP2K substrates, which could occur on an intra- or inter-molecular basis. Other partners also have distinct oligomeric states. For instance, Peroxiredoxin-1 has been demonstrated to transduce peroxide signals to ASK1 (50), and peroxiredoxin proteins frequently adopt ring-shaped decamers or dodecamers of five or six Prdx-1 dimers (51). Similarly, the phosphatase PGAM5 is known to target ASK1 (52), and structural studies have shown that PGAM5 forms dodecameric rings that are important for its activity on an ASK1 substrate peptide (53, 54). N-terminal regions of ASK1 have been shown to interact with TNF receptor-associated factor-type ubiquitin ligases (53), which form oligomers (55), and the F-box Cullin-ubiquitin ligase component Fbxo21 (54). Notably, the F-box protein FbxW11/βTrCP2 was also identified in our BiCAP analysis (table S3), further reinforcing cross-regulation between ASK complexes and the ubiquitin-proteasome system (56). Fbxo21 promotes Lys²⁹ (K29)-linked ubiquitylation on ASK1 during viral infection (32), on lysine residues near the binding site for 14-3-3 proteins. 14-3-3 proteins are themselves dimeric regulators of ASK proteins that bind C-terminal to the kinase domain (19). Ultimately, many of the regulatory interactions of ASK proteins could be exacerbated—or compete—in the context of full-length proteins that are tethered through their C-termini. Thus, there are multiple mechanisms by which ASK regulation—either autoinhibition or transactivation—stand to be enhanced by SAM domain-based oligomerisation.

Preferential hetero-oligomerisation between the ASK1 and ASK2 SAM domains is a relatively simple molecular mechanism to explain the greater efficacy of both proteins in eliciting stress responses in various settings than either protein alone (4–8). With isolated SAM domains, the heteromeric complex appears to be more stable than the homomeric

complex at equivalent concentrations, which if translated to full-length proteins would mean that higher-order active complexes form more readily and are more persistent. A key relevant question is how interactions by the C-terminal SAM domains relate to inter-kinase domain regulation that has previously been demonstrated between ASK1 and ASK2 (4). Several other additional questions remain, including whether other SAM domain-containing proteins may also be able to participate in ASK SAM oligomers. There was some incorporation of ASK3 into ASK1 complexes isolated during BiCAP; however, no other obvious SAM domain-containing candidates were identified (table S3). Regarding the propensity of the isolated ASK3 SAM domain to bind ASK1 and ASK2 SAM domains, GST pulldowns suggested that the monomeric ASK2 SAM domain could be bound by GST-ASK3 SAM domain, but the reciprocal interaction occurred less readily (Fig. 3A). Such behaviour might be explained by the stability of the ASK3 complex over a large concentration range. In equivalent experiments ASK1-ASK3 interactions appear less likely. However, whether ASK3 actively participates in endogenous ASK1-ASK2 complexes in cells is a relevant functional question.

Overall, this study uncovers a common protein-protein interaction domain that plays an important role in the function of ASK proteins—adding to the conserved repertoire of functional domains found in MAP kinases and their scaffolding proteins, from yeast to humans. These findings reinforce the modularity of signaling cascades in eukaryotes, in a manner that maintains remarkable specificity despite structural similarity. ASK proteins appear to be particularly rich in autoregulatory interaction domains, in line with their role at the intersection of many cellular stresses. Understanding how these features work in concert, at the protein level and in cells, remains an ongoing challenge relevant to this multipurpose signaling hub.

Materials and Methods

DNA Constructs

Tandem-tagged constructs for HEK293 expression and HNE induction (ASK1 (HA-Flag) and ASK2 (HA-V5) Addgene # 69726, #69727, respectively) were a kind gift from Daniel Liebler (55). For BiCAP experiments The pDONR223-MAP3K5 used (Addgene plasmid 23517) (57) was a kind gift of Dr William Hahn and Dr David Root. An expression vector encoding full length Venus fluorescent protein was a kind gift from Dr Stephen Michnick (University of Montreal). The ASK1 SAM domain was amplified from the MegaMan Transcriptome library (Agilent). Constructs comprising ASK2 and ASK3 were amplified from Addgene plasmids (#69727 and #69728, respectively). Indicated fragments were cloned into a pET-LIC vector either containing an N-terminal 6xHis or GST tag, and a 3C protease cleavage site. All mutants were generated using QuikChange mutagenesis using Q5 Polymerase (New England Biolabs) and verified by Sanger sequencing.

Protein Expression and Purification

All recombinant proteins were expressed in *E. coli* BL21(DE3) in LB media, induced with IPTG overnight at 18 °C, and lysed by sonication. ASK1 (1290–1374), ASK2 (1216–1288) and ASK3 (1241–1313) were initially purified from clarified *E. coli* lysate by Ni²⁺-affinity chromatography using HisSelect resin (Sigma), followed by size exclusion chromatography (Superdex 75 column; GE Healthcare), with a 3C cleavage step between. SEC was carried out using a buffer consisting of 10 mM HEPES (pH 7.6), 150 mM NaCl and 2 mM DTT. Purified proteins were snap frozen in aliquots using liquid nitrogen.

Analytical Ultracentrifugation

Sedimentation velocity experiments using absorbance optics were conducted in a Beckman XL-I analytical ultracentrifuge. Initial scans were performed at 3,000 rpm to determine the optimal wavelength for data collection. Experiments were conducted at 20 °C, the pre-determined wavelength, continuous mode, 50,000 rpm in 20 mM HEPES (pH 7.6), 150 mM NaCl 0.2 mM TCEP. Buffer density and viscosity and an estimate of the partial specific volume of proteins (\bar{v}) was calculated using SEDNTERP. Data were fitted to a continuous sedimentation coefficient [c(s)] model using SEDFIT. Data were visualised by creating c(s) vs. s graphs using the GUSI software.

Crystallisation and Structure Solution

ASK3(1241–1313) was initially crystallised in 0.1 M Bis-Tris pH 6.5, 25 % (w/v) PEG3350 at a 1:1 drop ratio. Optimisation was carried out using the Hampton Research stock options pH kit with diffracting crystals grown in 0.1 M sodium citrate tribasic dihydrate pH 5, 25 % (w/v) PEG3350, and frozen with the addition of 20% (v/v) glycerol. X-ray diffraction data were collected at the Australian Synchrotron beamline MX2. Native and iodide soaked (0.5 M NaI) crystals were collected at 0.9357 and 1.456 Å wavelengths, respectively. The structure was solved using single-wavelength anomalous dispersion, using a 1.8 Å dataset. The Auto-Rickshaw webserver was used for structure solution by generating initial phases and an electron density map (58). An initial model was built by Buccaneer and improved using cycles of automated and manual refinement using the PDB_REDO web server (59), Phenix (60) and Coot (61). Structural figures were generated using PyMOL (Schrodinger).

SEC-MALS

Samples were separated by SEC in a buffer consisting of 10 mM HEPES (pH 7.6), 150 mM NaCl, and 0.3 mM TCEP and loaded at 100 or 200 μ M. SEC-MALS scattering data was collected using a Wyatt Dawn 8+ detector (Wyatt Technology) connected in-line to the Superdex 75 10/300 column (GE Healthcare) and a refractive index detector. All data were analyzed using ASTRA V software.

Cell Lines and Cell Culture

HEK-293FT cells were grown in DMEM (Life Technologies, 10566) supplemented with 10% fetal bovine serum (Sigma-Aldrich, F8067), 2 mM L-glutamine (Life Technologies, 25030081), 100 units/mL Penicillin-Streptomycin (Life Technologies, 15140122), Non-Essential Amino Acids (Hyclone, SH30238) and 1 mM Sodium Pyruvate ((Hyclone, SH3023901). Cells were grown at 37 °C in a humidified atmosphere with 5% CO₂.

HNE Stimulation

Cells were transiently co-transfected with Lipofectamine 3000 (Life Technologies, L3000015). A total of 3 μ g plasmid DNA was used; either 1.5 μ g of relevant ASK construct and/or pcDNA3. Cells were grown for twenty-four hours before 4-hydroxy-2-nonenal (HNE) treatment. One hour before treatment the medium was replaced with serum free- media. Cells were treated with either ethanol (vehicle control) or 50 μ M HNE for 1 h at 37 °C. Cells were harvested into the treatment medium and centrifuged at 500 x g for 5 min at 4 °C. The cell pellets were washed twice with ice cold phosphate buffered saline (PBS) and the cell pellet resuspended in 100 μ L of 4x SDS-PAGE Sample Buffer. Samples were frozen in liquid nitrogen and stored at -80 °C until use.

GST Pulldowns

ASK1 (1290–1374), ASK2 (1216–1288) and ASK3 (1241–1313) were cloned as GST-fusion constructs and expressed in BL21(DE3) cells. Small-scale protein preparations (100 mL cultures) of GST-fusion proteins were lysed by sonication and the supernatant purified using glutathione-S-transferase (GSH) Sepharose beads (GE Healthcare) pre-equilibrated using phosphate-buffered saline (PBS). All GSH-bound constructs were incubated with each ASK1 (1290–1374), ASK2 (1216–1288) or ASK3 (1241–1313) purified as His-tagged proteins as described above. Isolated SAM domain was added in approximately five fold excess to GST-fusion, and samples were incubated for 20 minutes at 4 °C. GSH beads were washed four times with GST buffer and samples were analysed by SDS-PAGE.

Western Blotting

For analysis by western blot, samples were separated by SDS/PAGE and transferred to 0.2 μ m nitrocellulose (Life Technologies, IB23002). Membranes were blocked in 5% BSA (w/v) in TBS-T. Membranes were incubated with primary antibodies overnight at 4°C in 5% BSA (w/v) in TBS-T. Antibodies used in this study were rabbit monoclonal p38 MAPK (1:2000, CST, #8690), rabbit monoclonal Phospho-p38 MAPK (Thr180/Tyr182) (1:500, CST, #4511), Phospho-ASK1 (Thr845 in mouse, Thr838 in human ASK1) (1:1000, CST, #3765), mouse monoclonal V5 tag (1:5000, Abcam, ab27671), rabbit monoclonal DYKDDDDK tag (Flag tag, 1:1000, CST, #14793) and/or mouse monoclonal α -tubulin (1:10,000, Millipore, 05-829). Following three washes with TBS-T, membranes were incubated with secondary antibodies

diluted in TBS-T with 1% (w/v) BSA for 1 hour at room temperature. Secondary antibodies used were goat anti-rabbit IRdye 680LT (LI-COR), goat anti-mouse IRdye 800LT (LI-COR) or goat anti-rabbit HRP-conjugated (1:10,000, Abcam, ab6721; used with Phospho-p38 MAPK). Membranes were washed a further three times with TBS-T. Membranes were then developed with the Odyssey Fc imaging system.

Bimolecular complementation affinity purification

Vectors expressing V1 or V2 tagged fusions of ASK1 were generated by recombination cloning into pDEST-V1 or pDEST-V2 destination vectors using Gateway LR Clonase enzyme mix (Life Technologies) according to manufacturer's instructions and verified by sequencing.

HEK293T cells were grown in 10 cm dishes and transfected with 2.5 μg of each BiCAP construct using JETprime transfection reagent (Polyplus). After 16 h, cells were harvested by washing twice with warm PBS and then scraping on ice with ice-cold lysis buffer (50 mM Tris HCl pH 7.4, 150 mM NaCl, 1 mM EDTA, 1% (v/v) Triton X-100) supplemented with fresh EDTA-free protease inhibitor cocktail and 0.2 mM sodium orthovanadate. Samples were cleared by centrifugation at 18000 $\times g$ for 10 min at 4°C to remove cellular debris, prior to proceeding with affinity purification using GFP-Trap_A agarose beads (ChromoTek GmbH), trypsin digestion and nanoLC-MS/MS as previously described in detail (30, 31).

Small-Angle X-ray Scattering

SAXS data was collected using the SAXS/WAXS beamline at the Australian Synchrotron with an inline gel-filtration chromatography setup (65). Protein samples (ASK1 SAM 50 μL at 9.2 $\text{mg}\cdot\text{mL}^{-1}$; ASK2 SAM 90 μL at 8.5 $\text{mg}\cdot\text{mL}^{-1}$; ASK1+2 SAM 90 μL at 5.2 $\text{mg}\cdot\text{mL}^{-1}$; ASK3 SAM 50 μL at 8.3 $\text{mg}\cdot\text{mL}^{-1}$) were injected onto a Superdex 75 Increase 5/150 column and eluted in 10 mM HEPES pH 7.5, 150 mM NaCl, 5% glycerol and 0.2 mM TCEP at a flow rate of 0.5 $\text{mL}\cdot\text{min}^{-1}$. Protein was eluted from the column into a 1 mm diameter quartz capillary orthogonally aligned to the X-ray beam. The coflow system, providing sheath flow, was used to achieve stable laminar flow through the capillary reducing radiation damage (66). Data was collected at 285 K using an X-ray beam of 1.03 Å in wavelength and 2 s exposure times. X-ray scattering was measured by a Pilatus 1M or 2M detector (Dectris). Primary data reduction and buffer subtraction was performed onsite at the Australian Synchrotron using scatterBrain software developed in-house (Stephen Mudie, Australian Synchrotron). Data analysis was performed using Primus (67), GNOM (68), and Crysol (69) from the ATSAS package (69).

Supplementary Materials

Fig. S1. ASK3 SAM crystal packing

Fig. S2. Analysis of ASK3 SAM mutants

Fig. S3. Potential ASK1 oligomer interfaces

Fig. S4. ASK1-ASK2 individual mutant activity

Fig. S5. ML-EH complex comparisons

Fig. S6. Comparison of SAXS models to scattering data

Fig. S7. SAM helical assemblies

Table S1. Summary of AUC data

Table S2. Crystallographic data

Table S3. Summary of BiCAP mass spectrometry data

Table S4. SAXS Data Parameters

Table S5. Summary of SAXS data fit to possible oligomeric models

References and Notes

1. H. Ichijo, E. Nishida, K. Irie, P. ten Dijke, M. Saitoh, T. Moriguchi, M. Takagi, K. Matsumoto, K. Miyazono, Y. Gotoh, Induction of apoptosis by ASK1, a mammalian MAPKKK that activates SAPK/JNK and p38 signaling pathways. *Science*. **275**, 90–94 (1997).
2. K. Hattori, I. Naguro, C. Runchel, H. Ichijo, The roles of ASK family proteins in stress responses and diseases. *Cell Commun. Signal*. **7**, 9 (2009).
3. Y. Kawarazaki, H. Ichijo, I. Naguro, Apoptosis signal-regulating kinase 1 as a therapeutic target. *Expert Opin. Ther. Targets*. **18**, 651–664 (2014).
4. K. Takeda, R. Shimosono, T. Noguchi, T. Umeda, Y. Morimoto, I. Naguro, K. Tobiume, M. Saitoh, A. Matsuzawa, H. Ichijo, Apoptosis signal-regulating kinase (ASK) 2 functions as a mitogen-activated protein kinase kinase kinase in a heteromeric complex with ASK1. *J. Biol. Chem*. **282**, 7522–7531 (2007).
5. T. Okazaki, M. Higuchi, K. Takeda, K. Iwatsuki-Horimoto, M. Kiso, M. Miyagishi, H. Yanai, A. Kato, M. Yoneyama, T. Fujita, T. Taniguchi, Y. Kawaoka, H. Ichijo, Y. Gotoh, The ASK family kinases differentially mediate induction of type I interferon and apoptosis during the antiviral response. *Sci. Signal*. **8**, ra78–ra78 (2015).
6. T. Iriyama, K. Takeda, H. Nakamura, Y. Morimoto, T. Kuroiwa, J. Mizukami, T. Umeda, T. Noguchi, I. Naguro, H. Nishitoh, K. Saegusa, K. Tobiume, T. Homma, Y. Shimada, H. Tsuda, S. Aiko, I. Imoto, J. Inazawa, K. Chida, Y. Kamei, S. Kozuma, Y. Taketani, A. Matsuzawa, H. Ichijo, ASK1 and ASK2 differentially regulate the counteracting roles of apoptosis and inflammation in tumorigenesis. *EMBO J*. **28**, 843–853 (2009).
7. D. E. Place, P. Samir, R. Karki, B. Briard, P. Vogel, T.-D. Kanneganti, ASK Family Kinases Are Required for Optimal NLRP3 Inflammasome Priming. *Am. J. Pathol*. **188**, 1021–1030 (2018).
8. S. Tartey, P. Gurung, T. K. Dasari, A. Burton, T.-D. Kanneganti, ASK1/2 signaling promotes inflammation in a mouse model of neutrophilic dermatosis. *J. Clin. Invest*. **128**, 2042–2047 (2018).
9. I. Naguro, T. Umeda, Y. Kobayashi, J. Maruyama, K. Hattori, Y. Shimizu, K. Kataoka, S. Kim-Mitsuyama, S. Uchida, A. Vandewalle, T. Noguchi, H. Nishitoh, A. Matsuzawa, K. Takeda, H. Ichijo, ASK3 responds to osmotic stress and regulates blood pressure by suppressing WNK1-SPAK/OSR1 signaling in the kidney. *Nat. Commun*. **3**, 1285 (2012).
10. R. Loomba, E. Lawitz, P. S. Mantry, S. Jayakumar, S. H. Caldwell, H. Arnold, A. M. Diehl, C. S. Djedjos, L. Han, R. P. Myers, G. M. Subramanian, J. G. McHutchison, Z. D. Goodman, N. H. Afdhal, M. R. Charlton, GS-US-384-1497 Investigators, The ASK1 inhibitor selonsertib in patients with nonalcoholic steatohepatitis: A randomized, phase 2 trial. *Hepatology*. **67**, 549–559 (2017).
11. M. S. Stark, S. L. Woods, M. G. Gartside, V. F. Bonazzi, K. Dutton-Regester, L. G. Aoude, D. Chow, C. Sereduk, N. M. Niemi, N. Tang, J. J. Ellis, J. Reid, V. Zismann, S. Tyagi, D. Muzny, I. Newsham, Y. Wu, J. M. Palmer, T. Pollak, D. Youngkin, B. R. Brooks, C. Lanagan, C. W. Schmidt, B. Kobe, J. P. MacKeigan, H. Yin, K. M. Brown, R. Gibbs, J. Trent, N. K. Hayward, Frequent somatic mutations in MAP3K5 and

- MAP3K9 in metastatic melanoma identified by exome sequencing. *Nat. Genet.* **44**, 165–169 (2011).
12. Y. Hayakawa, Y. Hirata, H. Nakagawa, K. Sakamoto, Y. Hikiba, H. Kinoshita, W. Nakata, R. Takahashi, K. Tateishi, M. Tada, M. Akanuma, H. Yoshida, K. Takeda, H. Ichijo, M. Omata, S. Maeda, K. Koike, Apoptosis signal-regulating kinase 1 and cyclin D1 compose a positive feedback loop contributing to tumor growth in gastric cancer. *Proc. Natl. Acad. Sci. U. S. A.* **108**, 780–785 (2011).
 13. Y. Hayakawa, Y. Hirata, K. Sakitani, H. Nakagawa, W. Nakata, H. Kinoshita, R. Takahashi, K. Takeda, H. Ichijo, S. Maeda, K. Koike, Apoptosis signal-regulating kinase-1 inhibitor as a potent therapeutic drug for the treatment of gastric cancer. *Cancer Sci.* **103**, 2181–2185 (2012).
 14. P. Zhang, P.-X. Wang, L.-P. Zhao, X. Zhang, Y.-X. Ji, X.-J. Zhang, C. Fang, Y.-X. Lu, X. Yang, M.-M. Gao, Y. Zhang, S. Tian, X.-Y. Zhu, J. Gong, X.-L. Ma, F. Li, Z. Wang, Z. Huang, Z.-G. She, H. Li, The deubiquitinating enzyme TNFAIP3 mediates inactivation of hepatic ASK1 and ameliorates nonalcoholic steatohepatitis. *Nat. Med.* **62**, S47 (2017).
 15. J. T. Liles, B. K. Corkey, G. T. Notte, G. R. Budas, E. B. Lansdon, F. Hinojosa-Kirschenbaum, S. S. Badal, M. Lee, B. E. Schultz, S. Wise, S. Pendem, M. Graupe, L. Castonguay, K. A. Koch, M. H. Wong, G. A. Papalia, D. M. French, T. Sullivan, E. G. Huntzicker, F. Y. Ma, D. J. Nikolic-Paterson, T. Altuhaifi, H. Yang, A. B. Fogo, D. G. Breckenridge, ASK1 contributes to fibrosis and dysfunction in models of kidney disease. *J. Clin. Invest.* **128**, 4485–4500 (2018).
 16. G. Bunkoczi, E. Salah, P. Filippakopoulos, O. Fedorov, S. Müller, F. Sobott, S. A. Parker, H. Zhang, W. Min, B. E. Turk, S. Knapp, Structural and functional characterization of the human protein kinase ASK1. *Structure.* **15**, 1215–1226 (2007).
 17. G. Fujino, T. Noguchi, A. Matsuzawa, S. Yamauchi, M. Saitoh, K. Takeda, H. Ichijo, Thioredoxin and TRAF family proteins regulate reactive oxygen species-dependent activation of ASK1 through reciprocal modulation of the N-terminal homophilic interaction of ASK1. *Mol. Cell. Biol.* **27**, 8152–8163 (2007).
 18. J. F. Weijman, A. Kumar, S. A. Jamieson, C. M. King, T. T. Caradoc-Davies, E. C. Ledgerwood, J. M. Murphy, P. D. Mace, Structural basis of autoregulatory scaffolding by apoptosis signal-regulating kinase 1. *Proc. Natl. Acad. Sci. U. S. A.* **114**, E2096–E2105 (2017).
 19. O. Petrvalska, D. Kosek, Z. Kukačka, Z. Tosner, P. Man, J. Vecer, P. Herman, V. Obsilova, T. Obsil, Structural Insight into the 14-3-3 Protein-dependent Inhibition of Protein Kinase ASK1 (Apoptosis Signal-regulating kinase 1). *J. Biol. Chem.* **291**, 20753–20765 (2016).
 20. K. Miyakawa, S. Matsunaga, K. Kanou, A. Matsuzawa, R. Morishita, A. Kudoh, K. Shindo, M. Yokoyama, H. Sato, H. Kimura, T. Tamura, N. Yamamoto, H. Ichijo, A. Takaori-Kondo, A. Ryo, ASK1 restores the antiviral activity of APOBEC3G by disrupting HIV-1 Vif-mediated counteraction. *Nat. Commun.* **6**, 6945 (2015).
 21. L. Jaroszewski, L. Rychlewski, Z. Li, W. Li, A. Godzik, FFAS03: a server for profile-profile sequence alignments. *Nucleic Acids Res.* **33**, W284-8 (2005).

22. A. Sathyamurthy, S. M. V. Freund, C. M. Johnson, M. D. Allen, M. Bycroft, Structural basis of p63 α SAM domain mutants involved in AEC syndrome. *FEBS J.* **278**, 2680–2688 (2011).
23. L. Mariotti, C. M. Templeton, M. Raney, P. Paracuellos, N. Cronin, F. Beuron, E. Morris, S. Guettler, Tankyrase Requires SAM Domain-Dependent Polymerization to Support Wnt- β -Catenin Signaling. *Mol. Cell.* **63**, 498–513 (2016).
24. A. A. Riccio, M. McCauley, M.-F. Langelier, J. M. Pascal, Tankyrase Sterile α Motif Domain Polymerization Is Required for Its Role in Wnt Signaling. *Structure.* **24**, 1573–1581 (2016).
25. J. J. Kwan, N. Warner, T. Pawson, L. W. Donaldson, The solution structure of the *S.cerevisiae* Ste11 MAPKKK SAM domain and its partnership with Ste50. *J. Mol. Biol.* **342**, 681–693 (2004).
26. J. R. Schneider, J. P. Lodolce, D. L. Boone, An Ubiquitin-like Motif in ASK1 Mediates its Association with and Inhibition of the Proteasome. *J. Biochem. Pharmacol. Res.* **1**, 161–167 (2013).
27. H. Nagai, T. Noguchi, K. Homma, K. Katagiri, K. Takeda, A. Matsuzawa, H. Ichijo, Ubiquitin-like sequence in ASK1 plays critical roles in the recognition and stabilization by USP9X and oxidative stress-induced cell death. *Mol. Cell.* **36**, 805–818 (2009).
28. F. Qiao, J. U. Bowie, The many faces of SAM. *Sci. STKE.* **2005**, re7 (2005).
29. J. D. Federspiel, S. G. Codreanu, A. M. Palubinsky, A. J. Winland, C. M. Betanzos, B. McLaughlin, D. C. Liebler, Assembly Dynamics and Stoichiometry of the Apoptosis Signal-regulating Kinase (ASK) Signalingosome in Response to Electrophile Stress. *Mol. Cell. Proteomics.* **15**, 1947–1961 (2016).
30. D. R. Croucher, M. Iconomou, J. F. Hastings, S. P. Kennedy, J. Z. R. Han, R. F. Shearer, J. McKenna, A. Wan, J. Lau, S. Aparicio, D. N. Saunders, Bimolecular complementation affinity purification (BiCAP) reveals dimer-specific protein interactions for ERBB2 dimers. *Sci. Signal.* **9**, ra69 (2016).
31. J. F. Hastings, J. Z. R. Han, R. F. Shearer, S. P. Kennedy, M. Iconomou, D. N. Saunders, D. R. Croucher, Dissecting Multi-protein Signaling Complexes by Bimolecular Complementation Affinity Purification (BiCAP). *J. Vis. Exp.* (2018), doi:10.3791/57109.
32. Z. Yu, T. Chen, X. Li, M. Yang, S. Tang, X. Zhu, Y. Gu, X. Su, M. Xia, W. Li, X. Zhang, Q. Wang, X. Cao, J. Wang, Lys29-linkage of ASK1 by Skp1-Cullin 1-Fbxo21 ubiquitin ligase complex is required for antiviral innate response. *Elife.* **5**, 249 (2016).
33. T. Maruyama, T. Araki, Y. Kawarazaki, I. Naguro, S. Heynen, P. Aza-Blanc, Z. Ronai, A. Matsuzawa, H. Ichijo, Roquin-2 Promotes Ubiquitin-Mediated Degradation of ASK1 to Regulate Stress Responses. *Sci. Signal.* **7**, ra8 (2014).
34. T. Rajakulendran, M. Sahmi, I. Kurinov, M. Tyers, M. Therrien, F. Sicheri, CNK and HYP form a discrete dimer by their SAM domains to mediate RAF kinase signaling. *Proc. Natl. Acad. Sci. U. S. A.* **105**, 2836–2841 (2008).

35. Y. Wang, Y. Shang, J. Li, W. Chen, G. Li, J. Wan, W. Liu, M. Zhang, Specific Eph receptor-cytoplasmic effector signaling mediated by SAM–SAM domain interactions. *Elife*. **7**, e35677 (2018).
36. B. T. Harada, M. J. Knight, S.-I. Imai, F. Qiao, R. Ramachander, M. R. Sawaya, M. Gingery, F. Sakane, J. U. Bowie, Regulation of enzyme localization by polymerization: polymer formation by the SAM domain of diacylglycerol kinase delta1. *Structure*. **16**, 380–387 (2008).
37. C. N. Leettola, M. J. Knight, D. Cascio, S. Hoffman, J. U. Bowie, Characterization of the SAM domain of the PKD-related protein ANKS6 and its interaction with ANKS3. *BMC Struct. Biol.* **14**, 17 (2014).
38. D. A. Jacques, J. Trewella, Small-angle scattering for structural biology--expanding the frontier while avoiding the pitfalls. *Protein Sci.* **19**, 642–657 (2010).
39. M. C. Good, J. G. Zalatan, W. A. Lim, Scaffold proteins: hubs for controlling the flow of cellular information. *Science*. **332**, 680–686 (2011).
40. S. M. Coyle, J. Flores, W. A. Lim, Exploitation of Latent Allosterity Enables the Evolution of New Modes of MAP Kinase Regulation. *Cell*. **154**, 875–887 (2013).
41. R. P. Bhattacharyya, A. Reményi, M. C. Good, C. J. Bashor, A. M. Falick, W. A. Lim, The Ste5 scaffold allosterically modulates signaling output of the yeast mating pathway. *Science*. **311**, 822–826 (2006).
42. M. J. Knight, C. Leettola, M. Gingery, H. Li, J. U. Bowie, A human sterile alpha motif domain polymerizome. *Protein Sci.* **20**, 1697–1706 (2011).
43. M. K. Baron, T. M. Boeckers, B. Vaida, S. Faham, M. Gingery, M. R. Sawaya, D. Salyer, E. D. Gundelfinger, J. U. Bowie, An architectural framework that may lie at the core of the postsynaptic density. *Science*. **311**, 531–535 (2006).
44. C. A. Kim, M. L. Phillips, W. Kim, M. Gingery, H. H. Tran, M. A. Robinson, S. Faham, J. U. Bowie, Polymerization of the SAM domain of TEL in leukemogenesis and transcriptional repression. *EMBO J.* **20**, 4173–4182 (2001).
45. S. Horsefield, H. Burdett, X. Zhang, M. K. Manik, Y. Shi, J. Chen, T. Qi, J. Gilley, J.-S. Lai, M. X. Rank, L. W. Casey, W. Gu, D. J. Ericsson, G. Foley, R. O. Hughes, T. Bosanac, M. von Itzstein, J. P. Rathjen, J. D. Nanson, M. Boden, I. B. Dry, S. J. Williams, B. J. Staskawicz, M. P. Coleman, T. Ve, P. N. Dodds, B. Kobe, NAD⁺ cleavage activity by animal and plant TIR domains in cell death pathways. *Science*. **365**, 793–799 (2019).
46. M. Sporny, J. Guez-Haddad, M. Lebendiker, V. Ulisse, A. Volf, C. Mim, M. N. Isupov, Y. Opatowsky, Structural Evidence for an Octameric Ring Arrangement of SARM1. *J. Mol. Biol.* **431**, 3591–3605 (2019).
47. C.-F. Chuang, C. I. Bargmann, A Toll-interleukin 1 repeat protein at the synapse specifies asymmetric odorant receptor expression via ASK1 MAPKKK signaling. *Genes Dev.* **19**, 270–281 (2005).
48. D. Koveal, N. Schuh-Nuhfer, D. Ritt, R. Page, D. K. Morrison, W. Peti, A CC-SAM, for Coiled Coil-Sterile {alpha} Motif, Domain Targets the Scaffold KSR-1 to Specific Sites in the Plasma Membrane. *Sci. Signal.* **5**, ra94–ra94 (2012).

49. H. Lavoie, M. Sahmi, P. Maisonneuve, S. A. Marullo, N. Thevakumaran, T. Jin, I. Kurinov, F. Sicheri, M. Therrien, MEK drives BRAF activation through allosteric control of KSR proteins. *Nature*. **554**, 549–553 (2018).
50. R. M. Jarvis, S. M. Hughes, E. C. Ledgerwood, Peroxiredoxin 1 functions as a signal peroxidase to receive, transduce, and transmit peroxide signals in mammalian cells. *Free Radic. Biol. Med.* **53**, 1522–1530 (2012).
51. E. C. Ledgerwood, J. W. A. Marshall, J. F. Weijman, The role of peroxiredoxin 1 in redox sensing and transducing. *Arch. Biochem. Biophys.* **617**, 60–67 (2017).
52. K. Takeda, Y. Komuro, T. Hayakawa, H. Oguchi, Y. Ishida, S. Murakami, T. Noguchi, H. Kinoshita, Y. Sekine, S.-I. Iemura, T. Natsume, H. Ichijo, Mitochondrial phosphoglycerate mutase 5 uses alternate catalytic activity as a protein serine/threonine phosphatase to activate ASK1. *Proc. Natl. Acad. Sci. U. S. A.* **106**, 12301–12305 (2009).
53. K. Ruiz, T. M. Thaker, C. Agnew, L. Miller-Vedam, R. Trenker, C. Herrera, M. Ingaramo, D. Toso, A. Frost, N. Jura, Functional role of PGAM5 multimeric assemblies and their polymerization into filaments. *Nat. Commun.* **10**, 531 (2019).
54. A. Chaikuad, P. Filippakopoulos, S. R. Marcisin, S. Picaud, M. Schröder, S. Sekine, H. Ichijo, J. R. Engen, K. Takeda, S. Knapp, Structures of PGAM5 Provide Insight into Active Site Plasticity and Multimeric Assembly. *Structure*. **25**, 1089-1099.e3 (2017).
55. P. D. Mace, S. J. Riedl, Molecular cell death platforms and assemblies. *Curr. Opin. Cell Biol.* **22**, 828–836 (2010).
56. P. Filipčík, J. R. Curry, P. D. Mace, When Worlds Collide-Mechanisms at the Interface between Phosphorylation and Ubiquitination. *J. Mol. Biol.* **429**, 1097–1113 (2017).
57. C. M. Johannessen, J. S. Boehm, S. Y. Kim, S. R. Thomas, L. Wardwell, L. A. Johnson, C. M. Emery, N. Stransky, A. P. Cogdill, J. Barretina, G. Caponigro, H. Hieronymus, R. R. Murray, K. Salehi-Ashtiani, D. E. Hill, M. Vidal, J. J. Zhao, X. Yang, O. Alkan, S. Kim, J. L. Harris, C. J. Wilson, V. E. Myer, P. M. Finan, D. E. Root, T. M. Roberts, T. Golub, K. T. Flaherty, R. Dummer, B. L. Weber, W. R. Sellers, R. Schlegel, J. A. Wargo, W. C. Hahn, L. A. Garraway, COT drives resistance to RAF inhibition through MAP kinase pathway reactivation. *Nature*. **468**, 968–972 (2010).
58. S. Panjikar, V. Parthasarathy, V. S. Lamzin, M. S. Weiss, P. A. Tucker, Auto-rickshaw: an automated crystal structure determination platform as an efficient tool for the validation of an X-ray diffraction experiment. *Acta Crystallogr. D Biol. Crystallogr.* **61**, 449–457 (2005).
59. R. P. Joosten, F. Long, G. N. Murshudov, A. Perrakis, The PDB REDO server for macromolecular structure model optimization. *IUCrJ.* **1**, 213–220 (2014).
60. P. D. Adams, P. V. Afonine, G. Bunkóczi, V. B. Chen, N. Echols, J. J. Headd, L.-W. Hung, S. Jain, G. J. Kapral, R. W. Grosse-Kunstleve, A. J. McCoy, N. W. Moriarty, R. D. Oeffner, R. J. Read, D. C. Richardson, J. S. Richardson, T. C. Terwilliger, P. H. Zwart, The Phenix software for automated determination of macromolecular structures. *Methods*. **55**, 94–106 (2011).

61. P. Emsley, K. Cowtan, Coot: model-building tools for molecular graphics. *Acta Crystallogr. D Biol. Crystallogr.* **60**, 2126–2132 (2004).
62. N. M. Kirby, S. T. Mudie, A. M. Hawley, D. J. Cookson, H. D. T. Mertens, N. Cowieson, V. Samardzic-Boban, A low-background-intensity focusing small-angle X-ray scattering undulator beamline. *J. Appl. Crystallogr.* **46**, 1670–1680 (2013).
63. M. Foglizzo, A. J. Middleton, A. E. Burgess, J. M. Crowther, R. C. J. Dobson, J. M. Murphy, C. L. Day, P. D. Mace, A bidentate Polycomb Repressive-Deubiquitinase complex is required for efficient activity on nucleosomes. *Nat. Commun.* **9**, 3932 (2018).
64. E. J. Petrie, J. J. Sandow, A. V. Jacobsen, B. J. Smith, M. D. W. Griffin, I. S. Lucet, W. Dai, S. N. Young, M. C. Tanzer, A. Wardak, L.-Y. Liang, A. D. Cowan, J. M. Hildebrand, W. J. A. Kersten, G. Lessene, J. Silke, P. E. Czabotar, A. I. Webb, J. M. Murphy, Conformational switching of the pseudokinase domain promotes human MLKL tetramerization and cell death by necroptosis. *Nat. Commun.* **9**, 2422 (2018).
65. N. Kirby, N. Cowieson, A. M. Hawley, S. T. Mudie, D. J. McGillivray, M. Kusel, V. Samardzic-Boban, T. M. Ryan, Improved radiation dose efficiency in solution SAXS using a sheath flow sample environment. *Acta crystallographica. Section D, Structural biology.* **72**, 1254–1266 (2016).
66. P. V. Konarev, V. V. Volkov, A. V. Sokolova, M. H. J. Koch, D. I. Svergun, PRIMUS: a Windows PC-based system for small-angle scattering data analysis. *J. Appl. Crystallogr.* **36**, 1277–1282 (2003).
67. D. I. Svergun, Determination of the regularization parameter in indirect-transform methods using perceptual criteria. *J. Appl. Crystallogr.* **25**, 495–503 (1992).
68. D. Svergun, C. Barberato, M. H. J. Koch, CRY SOL – a Program to Evaluate X-ray Solution Scattering of Biological Macromolecules from Atomic Coordinates. *J. Appl. Crystallogr.* **28**, 768–773 (1995).
69. D. Franke, M. V. Petoukhov, P. V. Konarev, A. Panjkovich, A. Tuukkanen, H. D. T. Mertens, A. G. Kikhney, N. R. Hajizadeh, J. M. Franklin, C. M. Jeffries, D. I. Svergun, ATSAS 2.8: a comprehensive data analysis suite for small-angle scattering from macromolecular solutions. *J. Appl. Crystallogr.* **50**, 1212–1225 (2017).

Acknowledgements: We thank members of the Mace Laboratory for useful discussions and assistance, particularly Pavel Filipčík for X-ray crystallography assistance. Various plasmids were kind gifts from Daniel Liebler, William Hahn, David Root, and Stephen Michnick (See Methods). **Funding:** Supported by the Marsden Fund Council from Government funding, managed by Royal Society Te Apārangi; PDM was also supported by a Rutherford Discovery Fellowship administered by the Royal Society Te Apārangi. Support is also acknowledged from the Victorian State Government Operational Infrastructure Support, NHMRC IRISS grant (9000433), and NHMRC fellowships (1105754 and 1172929; to J.M.M.). This research was undertaken in part using the SAXS/WAXS beamline and the MX2 beamline at the Australian Synchrotron, part of ANSTO, and made use of the ACRF detector. We thank the New Zealand Synchrotron Group for facilitating access to the MX beamlines, and the Biomolecular Interaction Centre for AUC access. **Author contributions:** P.D.M. designed the project. S.J.T., J.L.B. A.E.B. J.M.C. and A.L.C. performed experiments and all authors analyzed data. P.D.M. wrote the initial manuscript with input from all authors. **Competing interests:** The authors declare that they have no competing interests. **Data and materials availability:** The structure of the ASK3 SAM domain has been deposited to the Protein Data Bank (PDB, <https://www.rcsb.org>) with accession code 6V0M. The mass spectrometry proteomics data have been deposited to the ProteomeXchange Consortium via the PRIDE partner repository (<https://www.ebi.ac.uk/pride/>) with the dataset identifier PXD017498. All other data needed to evaluate the conclusions in the paper are present in the paper or the Supplementary Materials.

Figure Legends

Fig. 1. ASK1, ASK2, and ASK3 C-terminal domains have different oligomerisation propensities. (A) Overview of the domain architecture and conservation of ASK1, ASK2, and ASK3. IUPred score indicates the likelihood of amino acid residues being intrinsically unstructured. (B) Size-exclusion chromatography of ASK1(1290–1374), ASK2(1216–1288), and ASK3(1241–1313), corresponding to the regions of the respective ASK proteins labelled as SAM domain in (A). (C) Sedimentation velocity (analytical ultracentrifugation, AUC) analysis of the ASK1, ASK2, and ASK3 SAM domains.

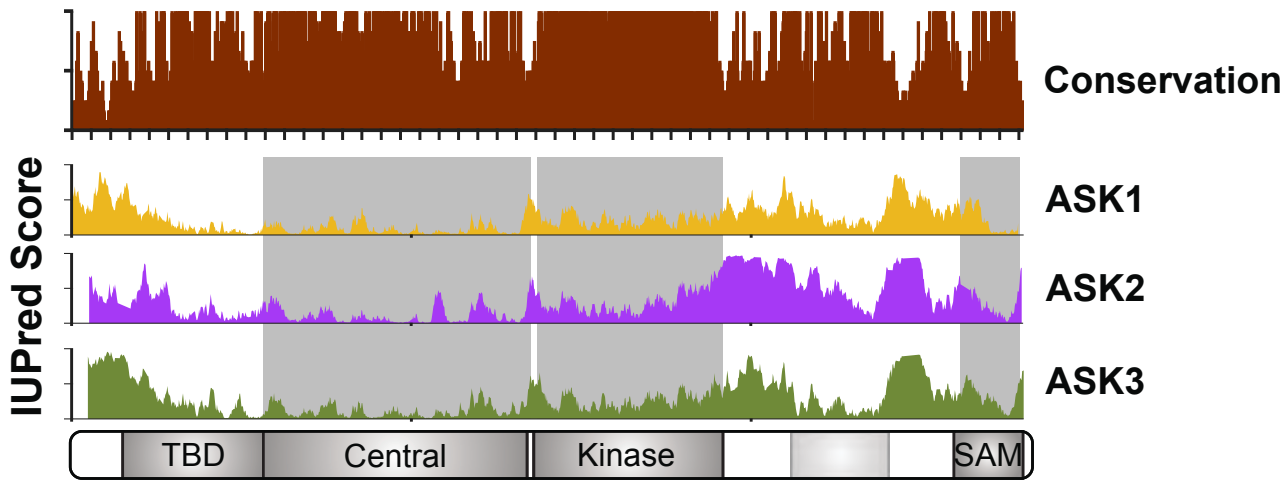
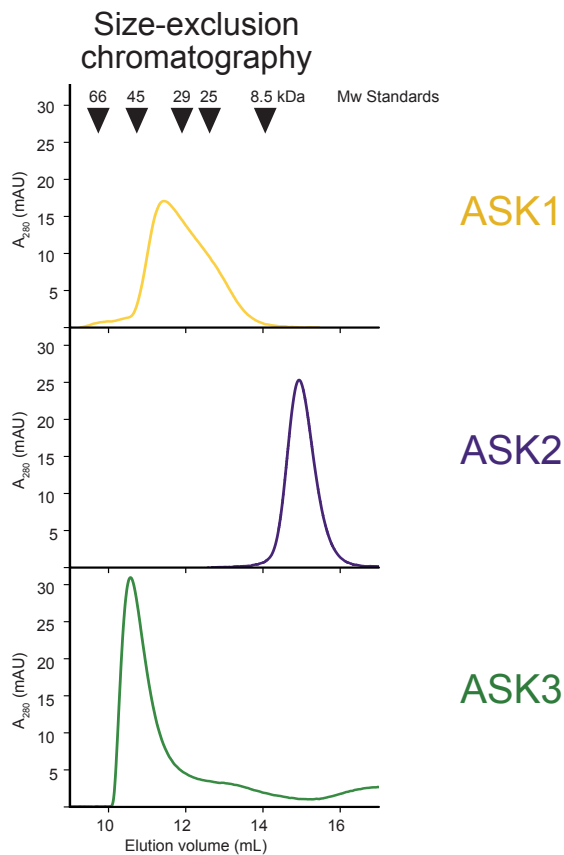
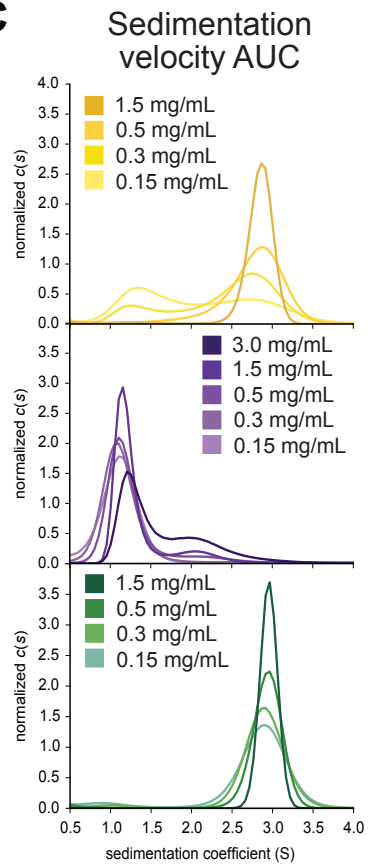
Fig. 2. Structure of the ASK3 SAM domain. (A) Cartoon representation of the crystal structure of ASK3(1241–1313) displaying the three monomers within the asymmetric unit. The ML-EH interface is indicated with dashed boxes. (B) Alignment of the SAM domains of human ASK1, ASK2, and ASK3. (C) Close-up view of wild-type residues within the dashed areas of the ML-EH interface. (D) Size-exclusion chromatography (SEC) trace for oligomers of wild-type (WT) and D1279K ASK3-SAM. (E) SEC-MALS data measuring the molar mass of oligomers formed by WT and C1291E ASK3-SAM.

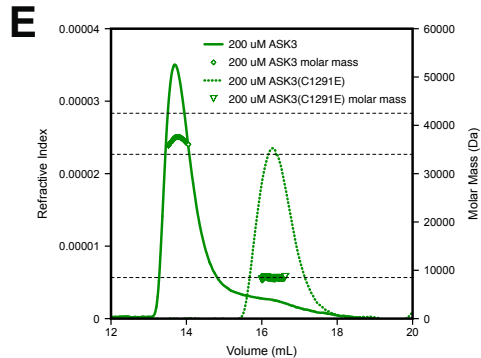
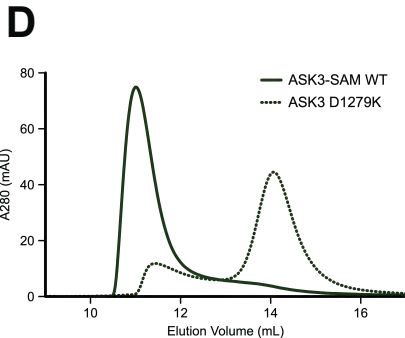
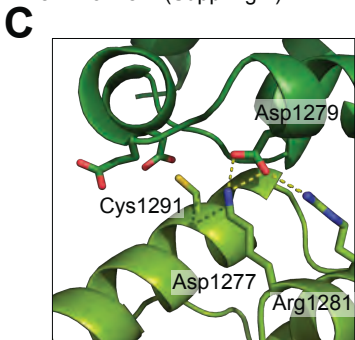
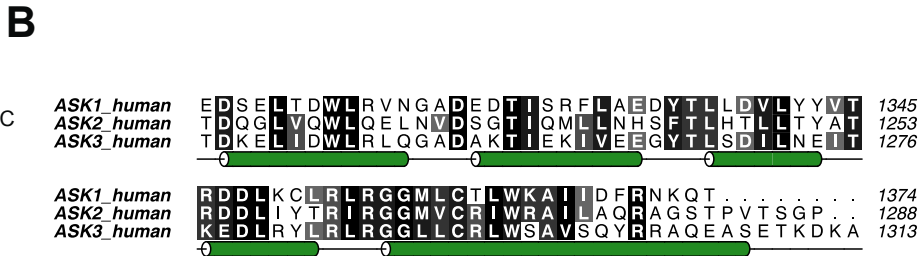
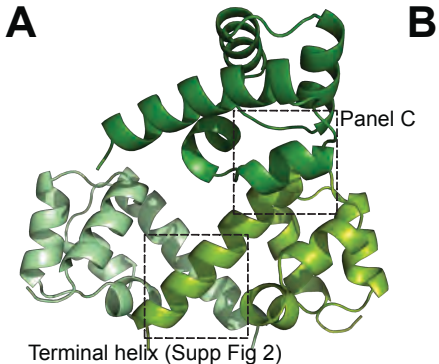
Fig. 3. Heterotypic interactions between ASK SAM domains. (A) Coomassie-stained gels of eluates from GST pulldown experiments measuring the ability of GST-ASK1, GST-ASK2, and GST-ASK3 SAM domains (bait) to pull down untagged SAM domains from ASK1, ASK2 and ASK3 (prey). $n = 2$ technical replicates. (B) Sedimentation velocity analytical ultracentrifugation of the isolated SAM domains of ASK1, ASK2, and an equimolar mixture of the two. (C) Coomassie-stained gel showing eluates from GST pulldown experiments measuring the ability of wild-type (WT) GST-ASK1 and GST-ASK2 SAM domains (bait) to pull down either WT or cysteine mutant forms of the ASK1 and ASK2 SAM domains. Image is representative of $n = 2$ technical replicates. (D) Analytical size-exclusion chromatography comparing the ability of WT and C1360E ASK1-SAM to form a higher-order oligomer with WT ASK2-SAM. (E) Analytical size-exclusion chromatography comparing the ability of WT and C1268E ASK2-SAM to form a higher-order oligomer with WT ASK1-SAM.

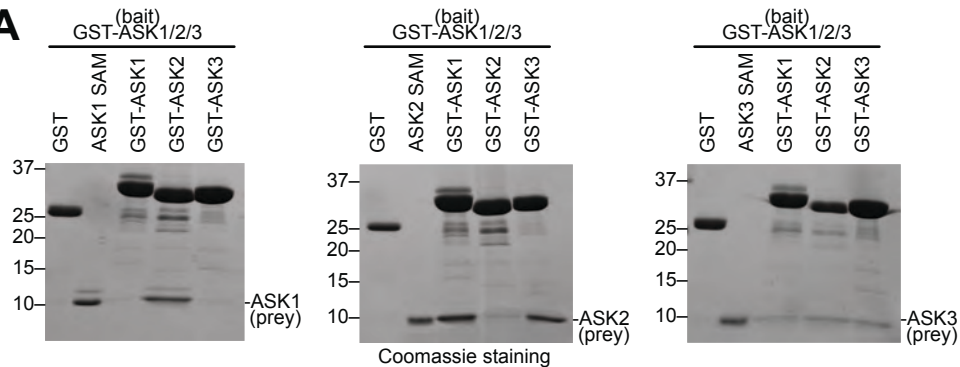
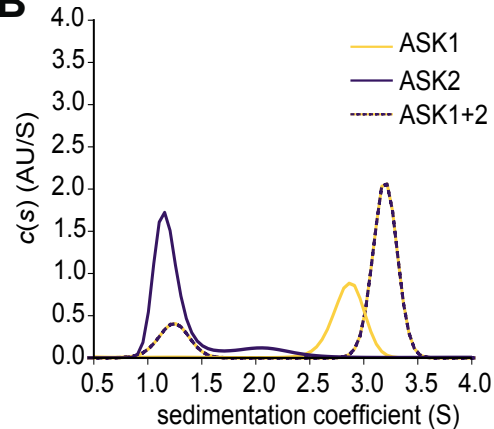
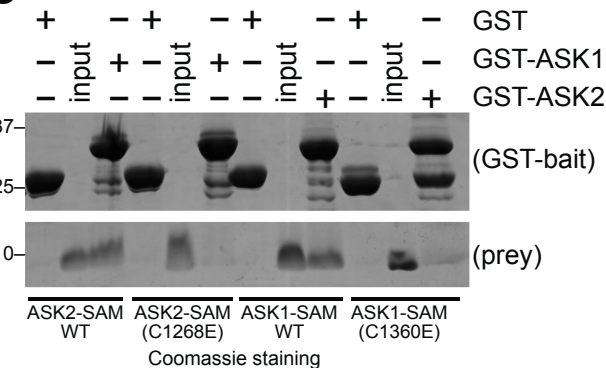
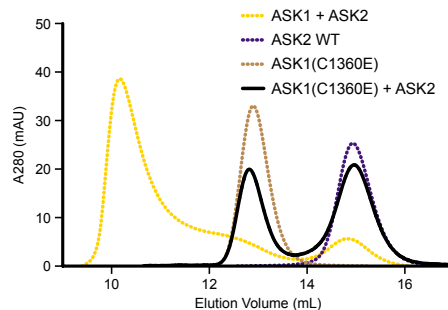
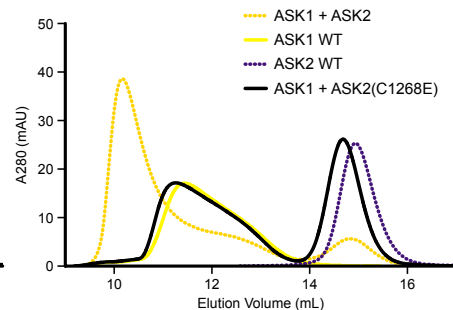
Fig. 4. Role of the ML-EH interface in ASK signaling and stoichiometry. (A) Western blotting of lysates from HEK293 cells expressing the indicated combinations of tagged, full-length WT ASK1 or ASK2 plus the corresponding untagged WT or cysteine mutant form of the respective protein, either unchallenged or challenged with HNE. Tubulin is a loading control. (B) Quantitation of the ratio between total ASK1, assessed by Flag immunoblotting in (A), and ASK1 phosphorylated on Thr⁸³⁸. Data points indicate individual ratios of four independent biological replicates, with the mean (bars) and standard error (error bars) of these points also indicated. (C) Schematic illustration of the BiCAP system as applied to ASK1. (D) Waterfall plot of BiCAP tandem mass spectrometry (MS/MS) data following immunoprecipitation with a nanobody specific for GFP. Data is expressed as the fold change over abundance calculated from a cell line transfected with GFP only and treated in an equivalent manner as a control. $n = 5$ technical replicates of each construct. (E) Analytical size-exclusion chromatography of mixtures containing indicated concentrations of the ASK1 and ASK2 SAM domains.

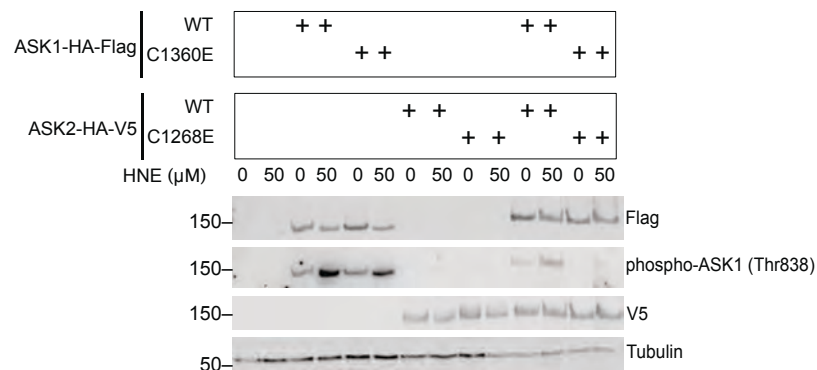
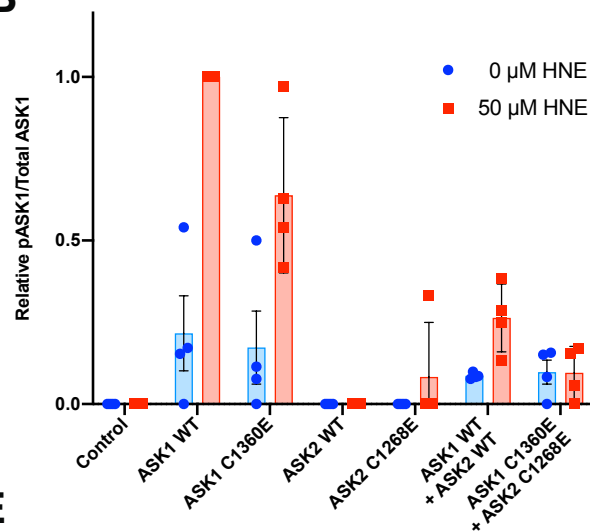
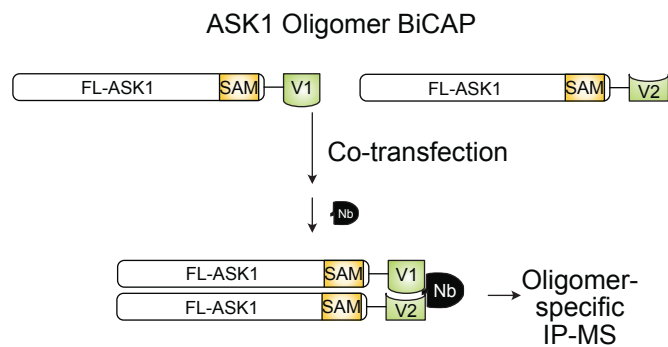
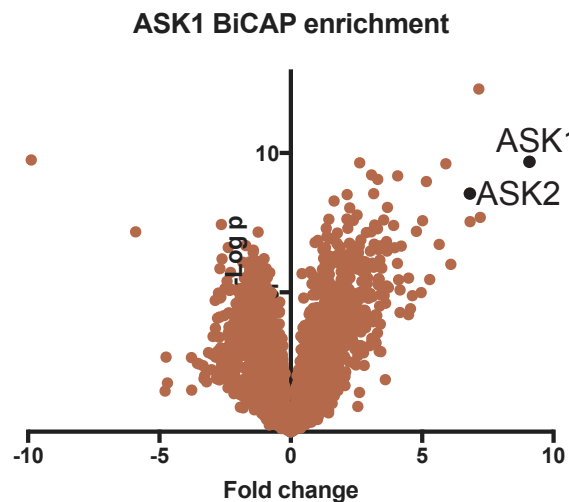
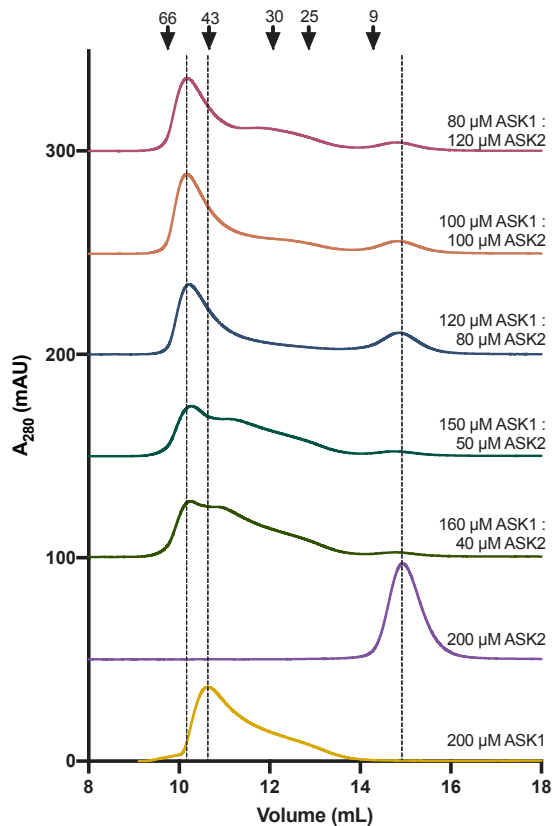
Fig. 5. The ASK SAM domain ML-EH interface (A) The greyscale schematic illustrates the interface formed between the mid-loop region (ML) of one ASK molecule and the end-helix region (EH) of another ASK molecule. The color surface representations show the electrostatic surfaces of ASK1, ASK2, and ASK3 SAM domains (as calculated using APBS (37)), with regions predicted to participate in ML-EH contacts outlined in yellow. The models of ASK1 and ASK2 were generated using MODELLER, based on the structure for the ASK3 SAM domain solved here. (B) Illustration of the ML-EH interface seen within the ASK3 asymmetric unit (ML-EH) and the similar but slightly offset arrangement with a crystallographically related SAM domain (ML-EH*). (C) Comparison of the ML-EH and ML-EH* interfaces. Pairs of SAM domains participating in each type of interface are overlaid based on the bottom SAM domain. Compared to the ML-EH interaction, the top SAM domain in the ML-EH* interaction is offset relative to the bottom SAM domain by an 18° shift of the $\alpha 5$ helix.

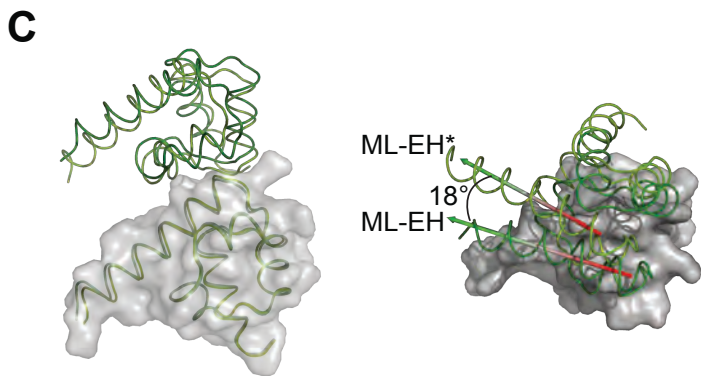
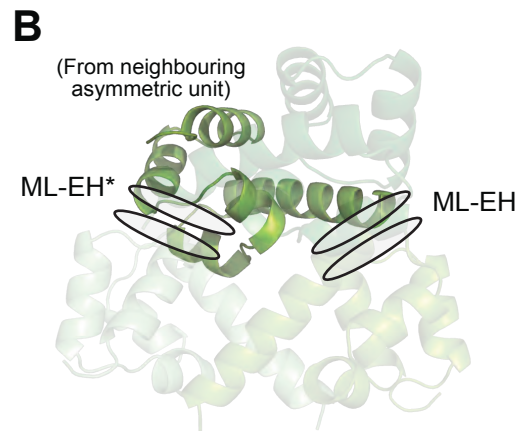
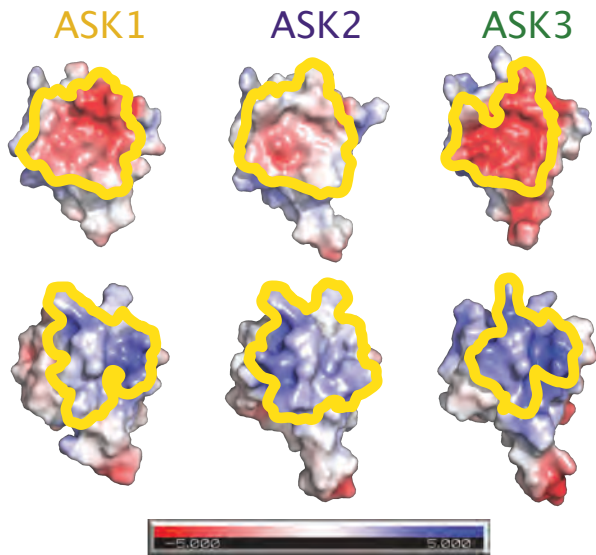
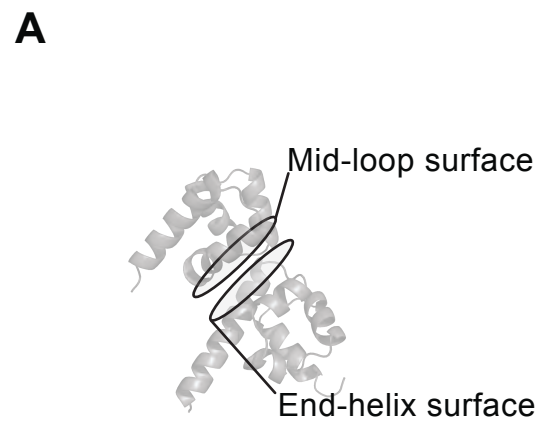
Fig. 6. SAXS analysis of ASK1+ASK2 and ASK3 SAM domains. (A) Schematic illustrating the possible helices modelled to be formed from the different ML-EH interfaces of the ASK3 SAM domain seen in the crystal lattice. Individual ASK3 SAM domains are colored in shades of green (B, C) Experimental scattering curves with the best CRY SOL modelled fit (black line) and the Guinier plot (inset) for, ASK1+ASK2 SAM hetero-oligomers (B) and ASK3 SAM homo-oligomers (C). (D, E) Distance distribution plots for ASK1+ASK2 SAM hetero-oligomers (D) and ASK3 SAM homo-oligomers (E). (F, G) Side and top views of best fit models for the ASK1+ASK2 SAM hexamer, with alternating ML-EH/ML-EH* interactions (F) and the ASK3 SAM hexamer, with repeated ML-EH interactions (G). (H) Summary of the fit of each model to the experimental SAXS data.

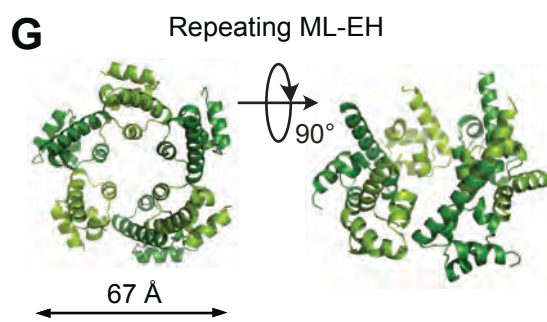
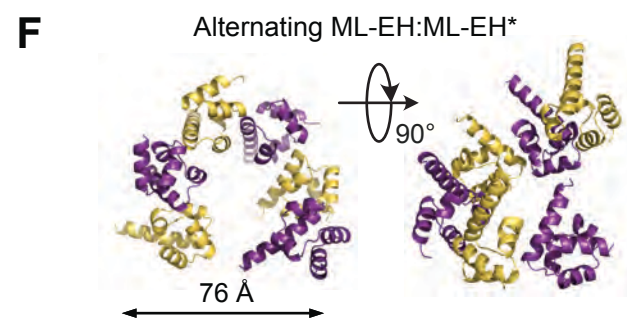
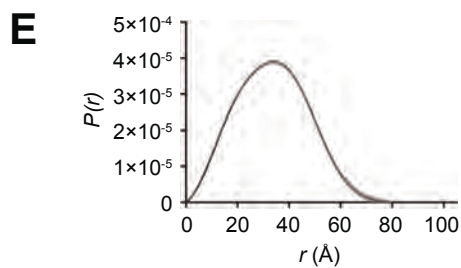
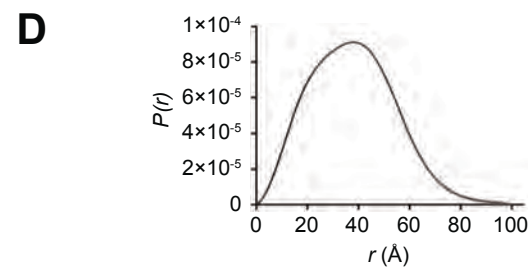
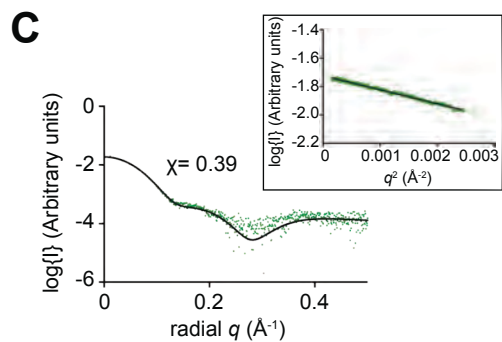
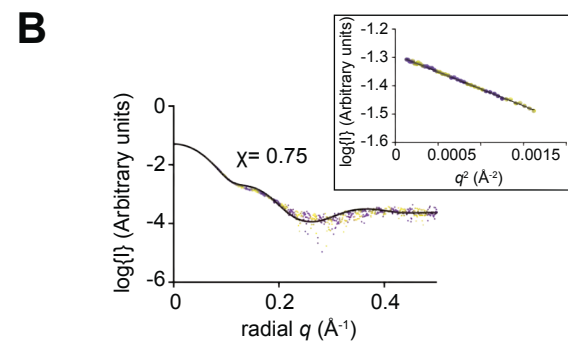
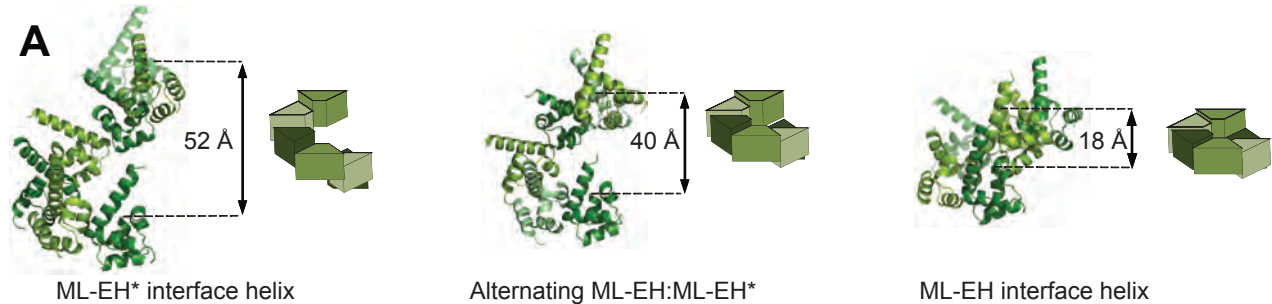
A**B****C**



A**B****C****D****E**

A**B****C****D****E**





H

	ML-EH* interface hexamer	Alternating ML-EH:ML-EH* hexamer	ML-EH interface hexamer
ASK1+2 SAM	$\chi = 0.75$	$\chi = 0.67$	$\chi = 0.97$
ASK3 SAM	$\chi = 0.96$	$\chi = 0.91$	$\chi = 0.39$